ARID ZONE JOURNAL OF ENGINEERING, TECHNOLOGY & ENVIRONMENT
AZOJETE June 2025. Vol.21(2):529-544
Published by the Faculty of Engineering, University of Maiduguri, Maiduguri, Nigeria.
Print ISSN: 1596-2490, Electronic ISSN: 2545-5818
https://doi.org/10.63958/AZOJETE/2025/21/02/018
www.azojete.com.ng

ORIGINAL RESEARCH ARTICLE

RESPONSE SURFACE MODELING OF SOURSOP RICH SEED PYROLYSIS FOR OPTIMUM BIO-OIL PRODUCTION

C. B. Ugwuodo [1*], H. U. Itiri [1], L. A. Enyinnaya[1], I. N. Emmanuel[2], S. E. Agbokwor[3], V.C. Uzoma[1], R.U. Daniel[1], and L.C. Ezeocha[1]

[1]*Department of Chemical Engineering, College of Engineering and Engineering Technology, Michael Okpara University of Agriculture, Umudike*
[2]*Department of Chemical Engineering, Nazarbayev University, Astana, Kazakstan*
[3] *Department of Mechanical Engineering, University of Nigeria Nsukka*
**Corresponding author's email: chijiokeugwuodo@mouau.edu.ng*

ARTICLE INFORMATION

Received: 19th March 2025
Revised: 1st May 2025
Accepted: 2nd May 2025

Keywords:
Bio-oil
Cellulose
Box benkhen design
Response surface methodology (RSM)
Soursop seed
Ultimization

ABSTRACT

This research investigates bio-oil production from soursop seed through pyrolysis, with process modelling and optimization conducted using RSM via Box-Benkhen design. Soursop seeds were oven-dried, ground, and sieved into various particle sizes within 1.0 to 6 mm range before undergoing pyrolysis at temperatures between 400 to 600 °C under inert nitrogen gas flow rates between 1.0 to 1.5 L/min. A Box-Behnken design under Response Surface Methodology (RSM) was used to model and optimize the effects of temperature, particle size, and inert gas flow on bio-oil yield. Proximate and ultimate analyses characterized the feedstock, while SEM revealed a porous structure favorable for pyrolysis. Bio-oil was characterized using FTIR and GC-MS to identify key functional groups and fatty acid composition. Proximate analysis showed the seeds had high volatile matter and fixed carbon, indicating good potential for pyrolysis. Ultimate analysis revealed carbon, hydrogen, nitrogen, oxygen, and sulphur contents of 51.29%, 5.90%, 0.50%, 42.30%, and 0.01%, respectively. Scanning Electron Microscopy (SEM) showed a rough, porous structure with oil-like droplets on the surface, which enhanced pyrolysis efficiency by providing a larger reactive surface area and improving devolatilization rates. The experimental design considered temperature, particle size, and gas flow rate combinations, with the bio-oil yield as the response. Results showed that increases in these parameters significantly affected bio-oil production. The maximum observed yield of 33.1% was achieved at 500°C, 6 mm particle size, and 1.0 L/min gas flow. The RSM model showed a high degree of fit with an R^2 value of 0.9875, adjusted R^2 of 0.9715, and predicted R^2 of 0.8007. Optimization predicted a maximum yield of 31.43% under conditions of 461.84°C, 3.84 mm particle size, and 1.02 L/min flow rate, with a desirability of 1.0. Experimental results closely matched these predictions, validating the model. Similarly, FTIR analysis indicates that the predominant monounsaturated fatty acid made up 45.55% of the total fatty acid content, which depicts that the oil belongs to the linoleic acid group. Furthermore, the FTIR analysis reveals that the alkene group contributes to increased reactivity and combustion efficiency, boosts the octane number of the bio-oil, and decreases the boiling point of the oil. Therefore, the FTIR and GC-MS analysis findings confirm that the bio-oil was within ASTM specifications.

1.0 Introduction

Biomass pyrolysis is a thermal decomposition process conducted in the absence of oxygen, converting organic materials into biochar, bio-oil, and syngas (Bridgwater, 2019). This process has gained significant attention due to its potential for producing renewable energy and high-value byproducts, which can mitigate the reliance on fossil fuels and contribute to a circular economy (Biswas *et al.*, 2022). Fixed-bed pyrolytic reactors are

prominent among the various pyrolysis technologies due to their simplicity, efficiency, and adaptability to different biomass feedstocks (Tripathi *et al*., 2021). Several methods are used today to create liquid fuel from biomass, including fermentation to produce ethanol (Hoover and Abraham, 2019), transesterification to produce biodiesel (Muley and Boldor, 2021) and pyrolysis to produce bio-oil (Goyal *et al.,* 2018). In a fixed-bed reactor, the biomass is placed in a stationary bed and heated, allowing for better control over the pyrolysis conditions (Mohan *et al*., 2021). This setup is particularly advantageous for studying the pyrolysis behaviour of specific biomass types, such as soursop seed (Wang *et al*., 2022). The fixed bed configuration ensures uniform heating and consistent product distribution, which are crucial for optimizing the pyrolysis process and enhancing the quality of the derived products (Wang *et al*., 2022).

Soursop (Annona muricata) is a tropical fruit celebrated for its nutritional and medicinal properties. Yet, its seeds are often overlooked and discarded as agricultural waste (Martínez *et al*., 2020). These seeds, which comprise about 20% of the fruit's total weight, contain valuable organic material that can be converted into useful products through pyrolysis (Ishaq *et al.,* 2020). The process involves heating the biomass in a fixed bed pyrolytic reactor, where it undergoes complex chemical reactions to produce solid (biochar), liquid (bio-oil), and gaseous products. (Zhao *et al*., 2023). The distribution and yield of these products are influenced by several factors, including temperature, heating rate, particle size, and residence time (Sharma *et al*., 2021). Recent studies have highlighted the potential of pyrolyzing soursop seeds as a sustainable waste management strategy and a method for generating renewable energy (Mansur *et al.,* 2020). The biochar produced from soursop seeds exhibits promising characteristics, such as high porosity and nutrient content, making it a potential candidate for soil amendment and carbon sequestration (Alkhalidi *et al.,* 2023). Moreover, bio-oil derived from the seeds can serve as a valuable source of biofuels and chemicals, aligning with the global shift towards greener energy solutions (Dajanta *et al.,* 2021).

Bio-oil derived from the pyrolysis of soursop seeds is rich in various organic compounds that can be upgraded to produce biofuels and bio-chemicals (Mansur *et al.,* 2020). The potential applications of bio-oil are extensive, ranging from energy production to the synthesis of high-value chemicals, thereby enhancing the economic viability of soursop seeds (Lehmann and Joseph, 2019). The temperature of pyrolysis plays a critical role in determining the composition and yield of the pyrolysis products (Aboelela *et al*., 2021). At lower temperatures (300-400°C), the process favours the production of biochar, while higher temperatures (500-700°C) increase the yield of bio-oil and syngas (Zhao *et al*., 2023). Soursop seed pyrolysis at varying temperatures has demonstrated this trend, where biochar yields decrease, and bio-oil yields increase with rising temperatures (Patel *et al*., 2021). Furthermore, the soursop seed's heating rate and particle size also influence the pyrolysis kinetics and product distribution (Dajanta *et al*., 2021). Faster heating rates enhance the bio-oil yield, while smaller particle sizes facilitate more efficient heat transfer and faster reaction rates (Huang *et al*., 2020). The pyrolysis of soursop seeds presents an environmentally friendly alternative to conventional waste disposal methods (Singh *et al*., 2021). By converting waste into energy and improving soil quality, pyrolysis contributes to the circular economy (Patel *et al*., 2021). Additionally, the process can help mitigate greenhouse gas emissions by sequestering carbon in the form of biochar (Alkhalidi *et al.,* 2023).

In search of optimal pyrolysis conditions, researchers explore modeling, predicting, and optimizing process parameters utilizing Responses Surfaces Methodology (RSM), (Ingie *et al*., 2023; Nwosu-Obieogu *et al*., 2024). RSM evaluates linear, interaction, and quadratic effects to identify ideal operating conditions for processes (Ude *et al*., 2020; Fakhari, 2023). While RSM has been used for pyrolysis of agricultural waste, there is currently a lack of literature on comprehensive investigations and optimization employing RSM, tailored explicitly for soursop seeds pyrolysis (Okeleye and Betiku, 2019; Belmajdoub and Abderaft, 2023).

Onaifo *et al*. (2023) investigated the co-pyrolysis of soursop and mango (*Mangifera indica*) seeds to produce high-quality bio-oil. Utilizing slow pyrolysis at temperatures between 350–500 °C with a heating rate of 5 °C/min and a residence time of 60 minutes, they achieved optimal bio-oil yields at 400 °C: 36.48% for soursop seeds, 20.54% for mango seeds, and 26.16% for the combined feedstock. Gas chromatography-mass spectrometry (GC-MS) analysis revealed that the co-pyrolyzed bio-oil was rich in hydrocarbons (41.16%), carboxylic acids (21.89%), ethers (13.60%), esters (7.99%), and phenolics (5.20%). The study concluded that co-pyrolysis suppressed ether formation, resulting in bio-oil with potential applications as a biodiesel substitute and in the industrial production of resins and adhesives. Schroeder *et al*. (2017) analyzed the liquid fractions obtained from the slow pyrolysis of soursop seed cake. The research focused on the chemical and physical properties, providing insights into their potential applications. Although specific details are limited, the study contributes to understanding the composition and utility of pyrolysis products derived from soursop seeds. Kan *et al*. (2016) reviewed the pyrolysis of lignocellulosic biomass, focusing on product properties and the influence of various pyrolysis parameters. Although not specific to soursop seeds, the study provides valuable insights into how factors such as temperature, heating rate, and residence time affect the yield and composition

Corresponding author's email address: chijiokeugwuodo@mouau.edu.ng

of biochar, bio-oil, and syngas, which can be applied to optimizing soursop seed pyrolysis processes. Sukumar et al. (2015) conducted rapid pyrolysis tests on sweet lime empty fruit bunches in a fixed bed reactor using an electric furnace to generate bio-oil. The impact of particle size, temperature and nitrogen gas flow rate on the end product yields were examined. These pyrolysis parameters are improved by Respond Surface Methodology (RSM) with a Box-Behnken Design (BBD). The findings demonstrated that the bio-oil yield is 28.3% for the experimental and 28.2% for the statistical approach at the optimal temperature of 550°C, 4mm of particle size, and 300 cm^3min^{-1} of gas flow rate.

Therefore, this work aims to optimize via RSM, implementing Box-Behnken on some selected parameters (temperature, particle size, and inert gas flow rate) that affect the pyrolysis of soursop seed. Furthermore, there is a need for more comprehensive studies on the environmental impacts of discarding this agricultural waste on the surroundings.

2. Materials and Method

2.1 Preparation of Feedstock

The soursop seed used in this study was obtained from a plantation in Ndoro village in the Ikwuano local government area of Abia State, Nigeria. The sample was thoroughly washed to remove all foreign materials and ensure it was free of impurities. The soursop seed was oven-dried for 48 hours at a controlled temperature (60-70°C) to a constant weight. The dried soursop seed was ground in a high-speed rotary cutting mill. The samples of ground soursop seeds were separated into various particle size distributions (1-6 mm) using a standard sieve and stored in different desiccators until needed.

2.1.1 Equipment used

The equipment used was an integration of different units and instruments. A stainless-steel reactor served as the primary vessel for thermal processing, securely sealed using a pair of flanges and spiral-wound gaskets to ensure leak-tight operation. Thermal insulation was provided by fiberglass wrapping, while precise temperature regulation was achieved using a K-type thermocouple connected to a digital temperature controller. Condensation of volatile products was facilitated through a water-cooled condenser connected downstream of the reactor. Additional components included nitrogen gas supplied from a pressurized cylinder to maintain an inert atmosphere, electric heaters for uniform heating, and fasteners (bolts and nuts) for secure assembly. Auxiliary tools such as a stopwatch, test sieves, and analytical balance were used for process timing, particle size classification, and mass measurements, respectively.

2.2 Characterization of the Feedstock

2.2.1 Proximate analysis

The proximate analysis is defined as the loss in weight of the soursop seed sample heated under the test condition specified. The proximate analysis was performed according to ASTM E871 and E872 to determine the soursop seed's moisture content (MC), volatile matter (VM), fixed carbon (FC), and ash content (AC). Equations 1, 2, 3 and 4 are used to deduce MC, VM, FC and AC respectively.

$$\text{Moisture content (wt \%)} = \left(\frac{Wo - W1}{Wo}\right) \times 100 \quad (1)$$

$$\text{Volatile matter (wt \%)} = \left(\frac{W1 - W2}{W1}\right) \times 100 \quad (2)$$

$$\text{Fixed carbon (wt \%)} = \left(\frac{W2 - W3}{W2}\right) \times 100 \quad (3)$$

where, W_o is the weight of sample in g before heating, W_1 is the weight of sample in g after heating at 115^0C, W_2 is the weight of sample in g after heating at 750^0C, W_3 is the weight of sample in g after heating at 900^0C. The mass of the ash will be calculated as a percentage of the original sample using Equation 4.

$$\text{Ash, mass \%} = \left(\frac{w}{W}\right) \times 100 \quad (4)$$

where, w = mass of ash (g) and W = mass of sample (g)

2.2.2 Ultimate analysis

Corresponding author's email address: chijiokeugwuodo@mouau.edu.ng

This test determines the element percent of carbon, hydrogen, nitrogen, sulphur, and oxygen in the soursop seed. The ultimate analysis was carried out in accordance with ASTM standards E777 and E778 for the determination of carbon, hydrogen, and nitrogen, respectively, as validated in previous studies (Demirbaş, 2004).

2.2.3 SEM (Scanning Electron Microscopy)

The morphological structure of the soursop seed was evaluated before paralyzing it using a scanning electron microscope (SEM) (JEOL-JSM 760F model, Japan) to investigate surface features at high magnification. The procedure involved collecting and cleaning mature seeds, air-drying them, sectioning them, drying them in a laboratory oven, mounting them on aluminum SEM stubs, applying a thin layer of gold to prevent charging, and imaging them under high vacuum. High-resolution micrographs were captured at various magnifications, observing surface features like texture, cracks, pores, and fibrous structures. The images were analyzed using SEM image analysis software to support further interpretation of the seed's structure and potential influence on pyrolysis behavior.

2.3 Experimental Procedures of the Fixed Bed Pyrolysis System

The pyrolysis of soursop seed was carried out in a lab-scale fixed-bed pyrolyzer. The reactor is made of a stainless steel tube with a height of 300 mm, an internal diameter of 94 mm, and an external diameter of 100 mm. We introduced 50 grams of soursop seeds, with particle sizes ranging from 1 mm to 6 mm, into the reactor for pyrolysis. The reactor was sealed with a lid and steam gasket to ensure gas impermeability. Nitrogen gas was purged downstream of the tubular reactor at a flow rate of 1.0, 1.25, and 1.5 L/min, respectively, to establish an inert atmosphere. We adjusted the electrical control panel to heat the heaters to 400, 500, and 600°C, respectively. A thermocouple was positioned at the reactor's apex to gauge the internal temperature. The reactor's temperature was periodically checked with a thermocouple as a safety measure. The volatile products created in the reactor were purged downward and flowed into the condenser. We established the condensation apparatus by immersing the filtering flask in cold water. The liquid oil and solid char were recovered separately, while non-condensable gas was vented into the atmosphere. This technique was repeated according to the number of runs specified in the experimental design. Each experiment ran for 30 minutes. We weighed the bio-oil and char using a digital scale, documented the results, and securely stored them in separate, well-sealed containers at room temperature. The yield percentages of pyrolysis products were determined using mass balance equations consistent with those reported in previous studies (Miandad *et al*., 2016; Bridgwater, 2012).

$$\%\, Yield\ of\ Bio-oil\ = \frac{X4 - X3}{\text{weight of feedstock}}\ \ X\ 100 \quad (5)$$

$$\%\, Yield\ of\ Biochar\ = \frac{X2 - X1}{\text{weight of feedstock}}\ \ X\ 100 \quad (6)$$

$$\%\, Yield\ of\ Biogas\ = 100 - (\%\ \text{yield of Bio-oil} + \%\ \text{yield of Biochar}) \quad (7)$$

where X_1 = Weight of empty reactor, X_2 = Weight of reactor after reaction, X_3 = Weight of empty measuring cylinder, X_4 = Weight of measuring cylinder with bio-oil.

2.4 Design of Experiment

The experimental design and statistical analysis were performed according to the RSM (Response surface methodology) using Design-Expert software (Version 13). Box-Behnken design was employed to study the combined effect of three independent variables, namely, temperature, particle diameter, and inert gas flow, on the yield and quality of the oil. A synthetic medium for bio-oil production by pyrolysis was optimized using the design of experiment and response surface methodology (RSM). The effects of components were investigated by the design of experiment. The statistical model was constructed via Box-Behnken design using the selected variables. The temperature, particle diameter, and inert gas flow was used as the independent variables and bio-oil yield was the response variables with 17 experimental runs.

Corresponding author's email address: chijiokeugwuodo@mouau.edu.ng

2.5 Characterization of Bio-oil

2.5.1 GC-MS (Gas Chromatography-Mass Spectrometry)

Gas chromatography-mass spectroscopy analysis was carried out on a Perkin Elmer Turbo Mass Spectrophotometer (Norwalk, CTO6859, and USA) incorporating a Perkin Elmer Auto sampler XLGC. The column utilized was Perkin Elmer Elite -5 capillary column measuring 30m × 0.25mm with a film thickness of 0.25mm consisting of 95% Dimethyl polysiloxane. The carrier gas employed was helium at a flow rate of 0.5 mL/min. A sample injection volume of 1µl was employed. The inlet temperature was sustained at 250°C. The oven temperature was initially set to 110°C for 4 minutes, followed by a rise to 240°C. Subsequently, set to escalate to 280°C at a rate of 20°C, concluding with a duration of 5 minutes. The total duration was 90 minutes. The MS transfer line was sustained at a temperature of 200°C. The source temperature was sustained at 180°C. GCMS was analyzed using electron impact ionization at 70 eV, and data was reviewed using total ion count (TIC) for compound identification and quantification. The spectra of the components were compared with the database of known component spectra recorded in the GC-MS library. Peak area measurements and data processing were conducted using Turbo-Mass OCPTVS-Demo SPL software.

2.5.2 FTIR (Fourier Transform Infrared Spectroscopy)

This study conducted a functional group analysis of the bio-oil utilizing Fourier transform infrared (FTIR) spectroscopy, Magna-IR550 (Nicolet, Madison). An online pen plotter was utilized with FTIR to generate the obtained liquids' infrared (IR) spectra. A minimal bio-oil will be applied to a potassium bromide (KBr) disc. The FTIR spectrum will be measured and recorded in the 500-3500 cm-1 region. The absorption frequency spectrum is recorded and plotted. The standard IR spectra of 61 organic compounds will be utilized to identify the functional groups present in the components of the generated bio-oil (Rajia *et al.,* 2023).

3. Results and Discussion

3.1 Results of Characterization of Soursop Seed

3.1.1 Proximate analysis result

Table 1 displays the proximate analysis results for the Soursop seed sample. The samples' values for ash content, moisture content, volatile matter, and fixed carbon were 3.75, 9.40, 15.97, and 70.88 (%w/w), respectively, while the energy value was 4480 kcal/kg. The Soursop seed proximate analysis showed that it contained more fixed carbon and volatile matter. These components are essential for oil production (Siqueira *et al*., 2008). The presence of low concentrations of moisture content and ash content favours the pyrolysis process considerably. This result is in close agreement with Abel *et al.* (2020); Pedro *et al.* (2022); and Anas *et al*. (2024).

Table 1: Proximate Analysis of the Soursop seed

Item	% value
Ash content	3.75 + 0.2
Moisture content	9.40 + 0.2
Energy Value (Kcal/kg)	4480
Volatile content	15.97+ 0.3
Fixed carbon content	70.88+ 0.2

3.1.2 Ultimate analysis result

The elemental compositions of the samples were evaluated by final analysis. As stated in Table 2, the values for Carbon, Hydrogen, Nitrogen, Oxygen, and Sulphur in the sample were 51.29, 5.90, 0.50, 42.30, and 0.01 mass% correspondingly. The elevated carbon and oxygen content signifies that soursop seed consists of highly polar structures, which is advantageous for the ion exchange adsorption mechanism. Similarly, the low sulfur and nitrogen content may mitigate the accumulation of hazardous compounds in the reactor compartment, reducing the pyrolysis plant's maintenance requirements. The low sulphur and nitrogen could lead to reduced SOx and NOx gases which severely impact the troposphere's ozone layer (Ayeni *et al*., 2018). This compared well with Ayeni *et al*., (2018); Anas *et al.* (2024); Narayan *et al.* (2021).

Corresponding author's email address: chijiokeugwuodo@mouau.edu.ng

Table 2: Ultimate Analysis of Soursop seed

Elements	Wt %
Carbon	51.29+ 0.1
Hydrogen	5.90 + 0.3
Nitrogen	0.50 + 0.2
Oxygen	42.30+ 0.1
Sulphur	0.01 + 0.2

3.1.3 Scanning electron microscopes (SEM) of Soursop seed

The morphology of the raw soursop seed was investigated by SEM, as shown in Plate 1, and the micrographs using a magnification of 8000x show a pore size of 100 μm. The surface area and pore volumes are very important factors because the material's degradation efficiency depends on their surface areas. The image has a rough surface with tiny pores and oil-like droplets on the surface. The surface area and pore volumes offered more significant areas of contact during pyrolysis reactions, making the material's rate of devolution faster. The seed's high surface area and oil-like droplets indicate a rich volatile content, contributing to higher bio-oil yield during pyrolysis. Greater pore volume allows for easier diffusion of volatile gases, reducing secondary cracking reactions and preserving desirable pyrolysis products. The material's surface roughness and porosity indicate rapid heat transfer and decomposition, enhancing thermal degradation efficiency, making it ideal for fast pyrolysis systems with short reaction times. This is similar to report of Abel *et al.* (2020); Adekanmi and Olowofoyeku, (2020).

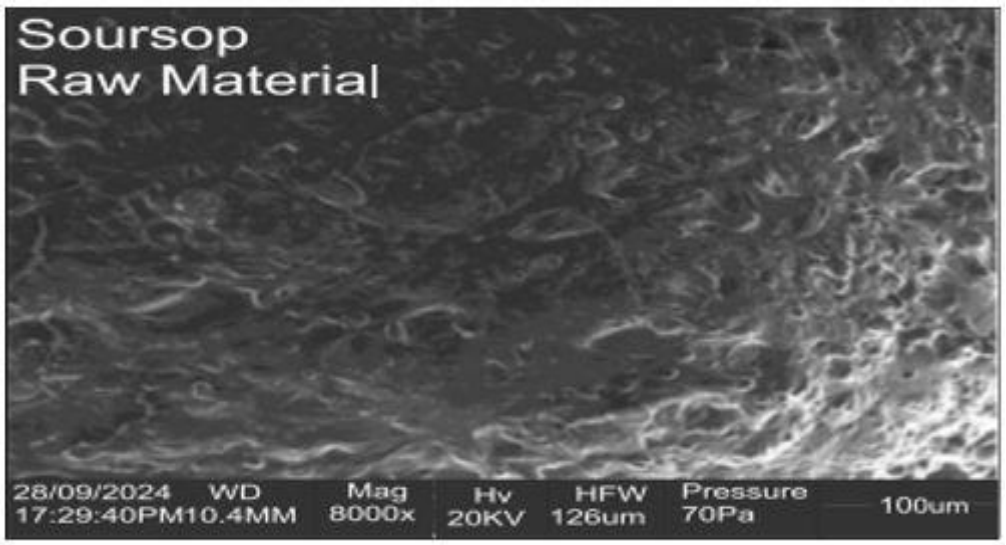

Plate 1: SEM micrographs of soursop seed

3.2 Results of Characterization of the Bio-Oil

3.2.1 Gas chromatography and mass spectrometry (GC-MS) analysis for the bio-oil

Figure 1 presents the bio-oil chemical composition achieved using GC-MS, and the concentration of these acids are as shown in Table 3. The compositions of the pyrolytic bio-oil were evaluated considering the relative peak area of identifying constituents using the obtained chromatogram from GC–MS analysis, which agrees with that presented by Laouge *et al.* (2020). The bio-oil has a total of eight peaks and is made up of Tetradecanoic Acid, Hexadecanoic Acid, Heptadecanoic Acid, 9- Octadecadienoic Acid, Octadecadienoic Acid, Eicosanoic Acid, Docosanoic Acid, and Heptacosanoic Acid. However, the most significant fatty acid in the bio-oil is 9, Octadecadienoic Acid (45.55%), Hexadecanoic Acid (27.80%), and Octadecadienoic Acid (24.30%), while Heptadecanoic Acid has the least concentration of 0.50%. Since linoleic is the predominant monounsaturated fatty acid and makes up 45.55% of the total fatty acid content, the oil belongs to the linoleic acid group (Sonntag, 2012). Linoleic acid is important for bio-oil applications because its chemical structure and properties contribute to fuel performance, stability, and reactivity. Its double bonds make it more prone to oxidation, contribute to lower pour points and better cold-flow properties, and during pyrolysis, linoleic acid produces a mix of hydrocarbons useful for biofuel applications, influencing bio-oil composition. This result compared well with the report of Okokpujie *et al.* (2023), Álvarez-Chávez *et al.* (2019), and Ude *et al.* (2023).

Corresponding author's email address: chijiokeugwuodo@mouau.edu.ng

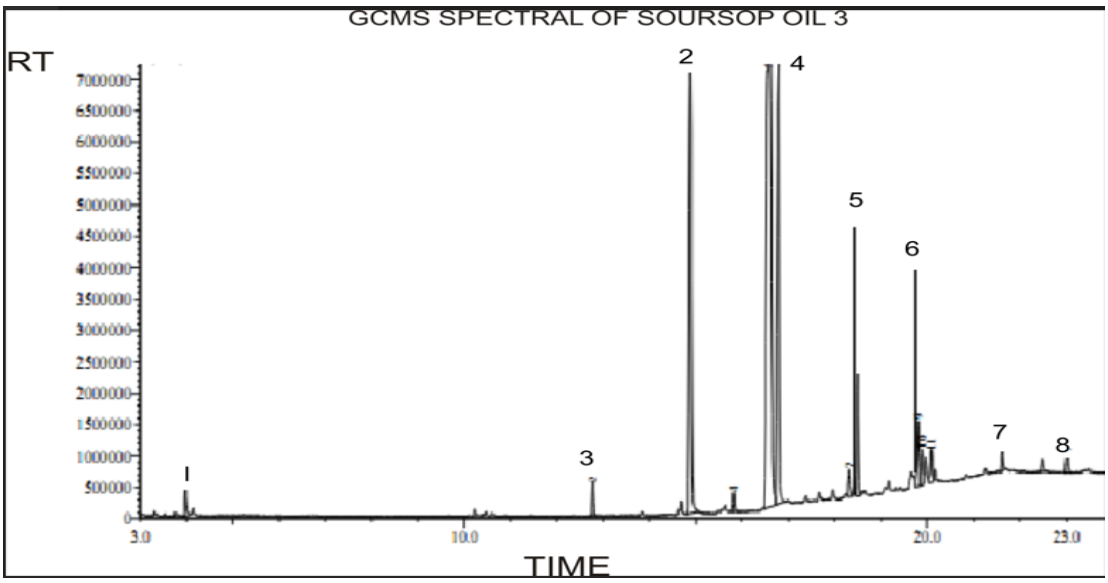

Figure 1: GC-MS of bio-oil compound produced from soursop seed

Table 3: Fatty acid composition of Soursop seed oil

S/No	Retention Time	Fatty Acid Present	Compound Names	Molecular Formular	% Concentration
1.	12.75	Tetradecanoic Acid	Myrisic Acid	$C_{14}H_{28}O_2$	0.90
2.	14.88	Hexadecanoic Acid	Palmitic Acid	$C_{16}H_{32}O_2$	27.80
3.	15.80	Heptadecanoic Acid	Margaric Acid	$C_{17}H_{34}O_2$	0.50
4.	16.60	9, Octadecadienoic Acid	Linoleic Acid	$C_{18}H_{31}O_2$	45.55
5.	16.80	Octadecadienoic Acid	Stearic Acid	$C_{18}H_{34}O_2$	24.30
6.	18.80	Eicosanoic Acid	Arachidic Acid	$C_{20}H_{40}O_2$	12.60
7.	20.10	Docosanoic Acid	Behenic Acid	$C_{22}H_{44}O_2$	1.05
8.	21.60	Heptacosanoic Acid	Cosnic Acid	$C_{27}H_{54}O_2$	0.65

3.2.2 FTIR analysis result of the bio-oil

Figure 2 depicts the FTIR spectrum of soursop seed oil. This research was undertaken to identify the different functional groups in the bio-oil. The investigation indicates the presence of =C-H functional groups (alkenes) at a precise frequency of 1036.2 cm^{-1}. They all display double-bonded bending-type vibrations within the spectrum's low energy and frequency range. They are ascribed to functional groups comprised of unsaturated olefinic chemicals (alkenes). These substances could be components of the methyl esters from unsaturated fatty acids found in bio-oil. The presence of the esters enhances combustion efficiency. It reduces particulate emissions, improves the fuel's lubricating properties, and is biodegradable and sourced from renewable feedstocks. Esters have minimal sulfur and aromatic content, lowering harmful emissions. The peaks detected at 1068.2 cm^{-1} are attributed to the stretching vibrations of the C-O and C-O-C molecules.

The band observed at 1378.2 cm^{-1} is associated with the bending vibrations of C=C bonds. In contrast, the band region at 1148.1 cm^{-1} is associated with the bending vibrations of C-H methyl groups. An assortment of fragrant chemicals is identified within the wavelength range of 1626.3cm^{-1}. The existence of the 2926.1 cm^{-1} area indicates the presence of a carboxylic acid with an elongated O-H group. The peaks observed at 2968.1 cm^{-1} indicate the symmetric stretching vibrations of the C-H alkane groups. Both methyl (CH_3) and methylene groups require substantial energy to generate stretching vibrations in their bonds. By contrast, alkene groups' usual C-H bending vibrations are detected at lower energy and frequency ranges. The peak observed at 3390.2 cm^{-1} is ascribed to the stretching vibration of alkene groups with =C-H bonds. The alkene group provides higher reactivity and combustion efficiency, enhances the bio-oil's octane number and lowers the oil's boiling point. This result aligns with the report of Ishaq *et al.* (2020).

Corresponding author's email address: chijiokeugwuodo@mouau.edu.ng

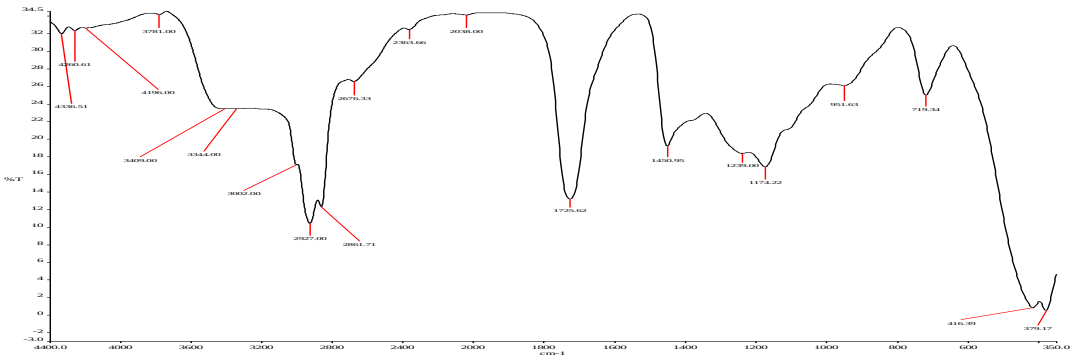

Figure 2: FT-IR spectrum of Pyrolysis of soursop seed for bio-oil

3.3 Response Surface Methodology Modeling For Bio-Oil Yield

The RSM- BBD results for the percentage yield of bio-oil from the pyrolysis process are presented in Table 4. Using design expert software version 13.0.6 USA, three variables, temperature, particle size, and gas flow rate represented by the alphabet A, B, and C, and three levels (-1, 0, and +1) were considered, resulting in seventeen experimental runs. The variation in values of the percentage yield of bio-oil indicated that the process parameters significantly affect the pyrolysis process. The maximum percentage yield of 33.1% occurred at a temperature of 500^{0}C, particle size diameter of 6mm, and inert gas flow rate of 1.0L/min. Second-order polynomial (quadratic) equations in coded terms that defined the independence between the studied process variables (A, B, C) and the response (% yield) for bio-oil were obtained with the use of RSM and represented in Equations (8).

Table 4: BBD experimental design for bio-oil yield

		Factor 1	**Factor 2**	**Factor 3**	**Response 1**
Std	Run	A:Temperature C	B:Particle size Mm	C:Inert gasflow L/min	Oil yield %
10	1	500	6	1	33.1
6	2	600	4	1	30
8	3	600	4	1.5	20.9
15	4	500	4	1.25	27.4
11	5	500	1	1.5	21
14	6	500	4	1.25	27.4
9	7	500	1	1	37
13	8	500	4	1.25	27.4
7	9	400	4	1.5	16.25
3	10	400	6	1.25	22.3
12	11	500	6	1.5	30.9
2	12	600	1	1.25	27.8
17	13	500	4	1.25	27.4
5	14	400	4	1	25.9
4	15	600	6	1.25	22
16	16	500	4	1.25	27.4
1	17	400	1	1.25	17.2

3.3.1 Oil yield model statistical analysis

Analysis of variance (ANOVA) was used to determine the statistical significance of the model and all the regressed coefficients of the developed quadratic RSM-BBD model for the % of bio-oil yield. The ANOVA results for measuring model adequacies for bio-oil yield are shown in Table 5. The high F – value (61.67), P-value (<0.0001), and non-significant lack of fit (*p-value*> 0.05) indicated that the model was significant (Hidayat *et al*., 2023).

The fitness of the model was expressed by the coefficient of determination (R^2) obtained as 0.9875 with an adjusted R^2 value of 0.9715, which was in reasonable agreement with the predicted R^2 value of 0.8007 for the developed model, i.e., the difference is less than 0.2. This showed that the developed quadratic model could predict the observed experimental data within the range of study (Kamarudin *et al.,* 2019). The adequate precision value of 30.8050, a measure of the signal-to-noise ratio greater than 4, showed the model's desirability and indicated an adequate signal. These regression values agreed with the report of (Malatji *et al.,*

2020), who suggested that a high correlation confirms the degree of fitness between the predicted and experimental responses. Therefore, this model can be used to navigate the design space.

The linear terms (A and C), the quadratic terms (A^2, B^2, and C^2), and the interactive effects of temperature: particle diameter (AB and BC) were all significant ($p < 0.05$) in the oil yield response model. As the process parameters increased, the positive and negative signs in Equation 8 showed an increase and decrease in values of response. Increased A, B, C, AB, AC, and BC led to increased response, while increased A2, B2, and C2 values resulted in decreased response. To check for the normality of the residuals, the normal probability versus studentized residuals plot was considered in Figure 3a. It showed that the points extended well diagonally, suggesting they dispersed in a reasonable pattern. The relationship between the predicted and observed actual experimental data in Figure 3b gave a straight line, which showed agreement with each other. Hence, the experimental data is acceptable (Reglioua *et al*., 2021).

Table 5: ANOVA results for BBD-RSM Bio-oil Yield

Source	Sum of Squares	df	Mean Square	F-value	p-value	
Model	471.70	9	52.41	61.67	< 0.0001	significant
A-Temperature	45.36	1	45.36	53.37	0.0002	
B-Particle size	3.51	1	3.51	4.13	0.0816	
C-Inert gasflow	170.66	1	170.66	200.80	< 0.0001	
AB	29.70	1	29.70	34.95	0.0006	
AC	0.0756	1	0.0756	0.0890	0.7741	
BC	47.61	1	47.61	56.02	0.0001	
A^2	159.58	1	159.58	187.76	< 0.0001	
B^2	4.92	1	4.92	5.79	0.0470	
C^2	17.16	1	17.16	20.19	0.0028	
Residual	5.95	7	0.8499			
Lack of Fit	5.95	3	1.98			not significant
Pure Error	0.0000	4	0.0000			
Cor Total	477.65	16				
Std. Dev.	0.9219	**R^2**	0.9875			
Mean	25.96	**Adjusted R^2**	0.9715			
C.V. %	3.55	**Predicted R^2**	0.8007			
		Adeq Precision	30.8050			

Oil Yield (%) = +27.40 + 2.38A +0.6625B - 4.62C - 2.73AB + 0.1375AC + 3.45BC - 6.16A^2 + 1.08B^2 + 2.02C^2 (8)

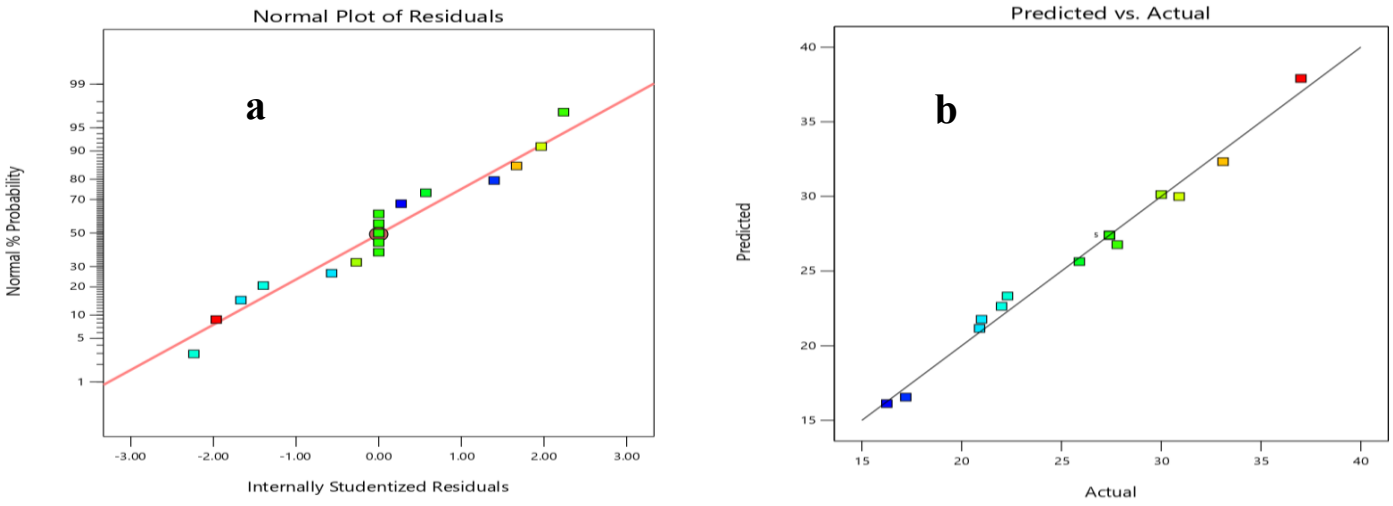

Figure 3: (a) Normal % probability vs. internal studentized residuals. (b) Predicted vs. Actual values

3.3.2 Interaction Effects of Process Parameters on Bio-oil Yield

To better understand the pyrolysis process for oil yield, contour and 3D response surface plots were studied. These plots were used to study the interaction effects of the pair of independent variables, keeping other variables constant. The 3D response surface plots are the graphical representation of the regression equation used to observe the levels of each factor (Mabrouka *et al.,* 2023). The interactive terms considered are

temperature and particle diameter (AB), temperature and inert gas flow (AC), and particle diameter and inert gas flow (BC). The interaction between temperature and particle diameter (AB) at the fixed inert gas flow on the % yield of bio-oil is shown in Figure 4. The maximum percentage (28.8%) of bio-oil yield was achieved at a temperature of 550 ^{0}C and a particle diameter of 1mm. At temperature levels >400^{0}C, a steady, significant increase in bio-oil yield was observed from particle diameter 1 mm to 6 mm. In contrast, no significant increase in yield was observed at temperature levels > 550^{0}C. Hence, an increase in AB up to A=550^{0}C and B =6 mm increased by % of bio-oil yield. This may be attributed to the fact that below the point of 400^{0}C the devolatilization of the feedstock has not started in full force. At this point, depolymerization is still occurring. A similar trend was recorded by Ganapathy *et al.* (2009). Figure 5 shows the contour and 3D surface response plot interaction of the combined effect of temperature and inert gas flow rate (AC) of bio-oil yield. Increase in A resulted in an increase % yield of bio-oil up to 550 ^{0}C after which the yield started decreasing gradually, while increase in B resulted in a significant decrease in the yield of the bio-oil. This may be as result of complete devolatilization of the biomass at the temperature level of 550 ^{0}C and the ability of the gas to purge the volatile oil out of the condenser before condensation takes place. This correspond to work done by Álvarez-Chávez *et al.* (2019). The interaction between particle diameter and inert gas flow rate (BC) was presented in Figure 6. An increase in BC resulted in a decrease in % yield of bio-oil. While the decrease is insignificant for an increase in particle size, it is significant for an increase in inert gas flow. This may be because complete devolatilization of the biomass has occurred, and at this point, secondary cracking of the biomass only leads to the formation of more gases and char, similar to the report of (Álvarez-Chávez *et al.*, 2019).

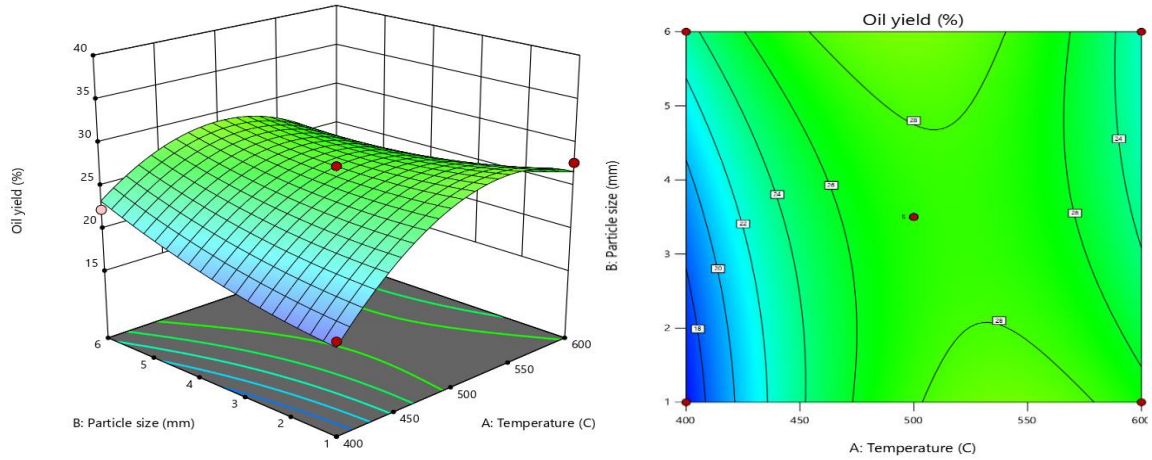

Figure 4: Contour and 3D plots on the effect of particle diameter and temperature on bio-oil yield

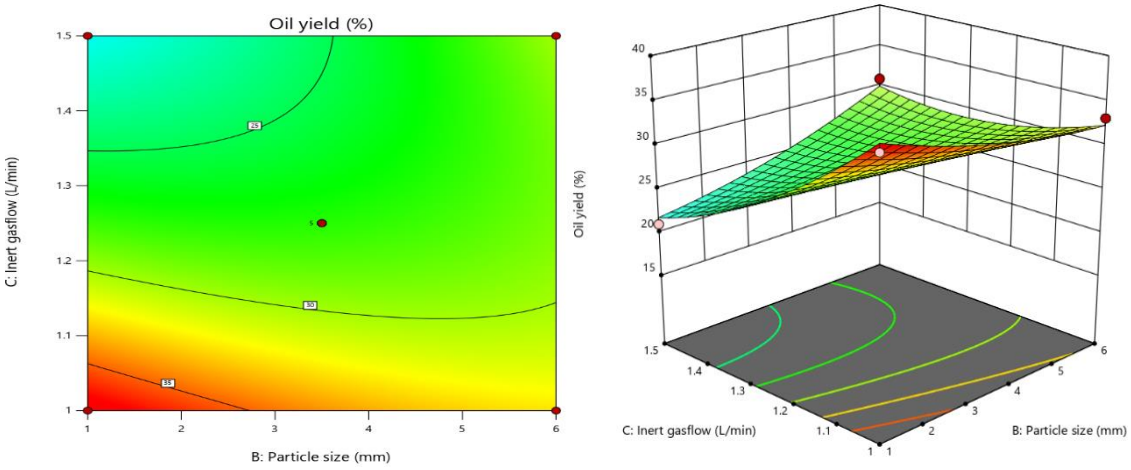

Figure 5: Contour and 3D plots on the effect of inert gas flow and temperature on bio-yield

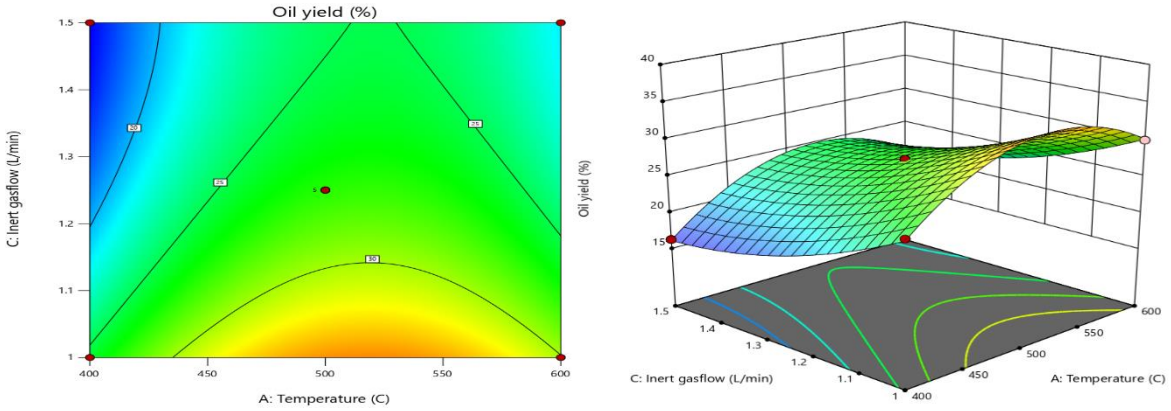

Figure 6: Contour and 3D plots on the effect of inert gas flow and particle diameter on bio-oil yield

3.4 Optimization of the Process

Table 6 visualizes the optimization criteria set on the Design Expert software to achieve maximum yield and purity responses. The software default weighted coefficient for both independent and dependent variables was tabulated accordingly in Table 6. Temperature, particle diameter and inert gas flow were fixed within their experimental ranges of 400-600°C, 1-6 mm, and 1.5-1.5 L/min respectively, and the oil yield were optimized within the range.

The optimum operating region for yield optimization was obtained using the desirability function algorithm of Box Behnken design. Figure 7 shows values of 461.84°C, 3.84mm, and 1.02L/m as the optimum mixture for temperature, particle size, and inert gas flow, respectively. These values give optimum yield responses (31.43%) with a desirability of 1.

Figure 8 presents the desirability values of the optimized condition for optimization of the bio-oil and biochar yield. It shows 1, 1, 1, and 1 as desirability values of temperature, particle size diameter, inert gas flowrate, and oil yield, respectively, 1 was obtained as combined desirability. The combined desirability for n number of responses is obtained from Equation 9.

$$D(x) = (d_1 \times d_2 \times \ldots . d_n)^{1/n} \quad 9$$

Table 7 gives the first 10 optimum conditions, responses to bio-oil and biochar yield, and the desirability for the criteria indicated in Table 7. For this current study, the first of the solutions was adopted.

Table 6: Constraints for optimization of yield and purity responses.

Name	Goal	Lower Limit	Upper Limit	Lower Weight	Upper Weight	Importance
A: Temperature	is in range	400	600	1	1	3
B: Particle diameter	is in range	1	6	1	1	3
C: Inert Gas flow	is in range	1	1.5	1	1	3
Oil yield	is in range	16.25	37	1	1	3

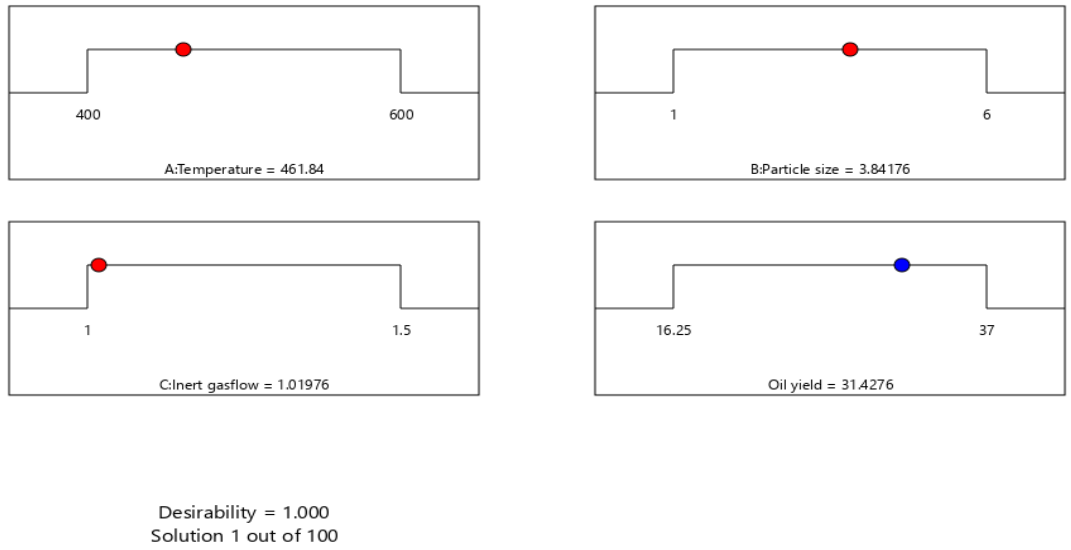

Figure 7: Numerical optimized value of the dependent and independent variables with desirability

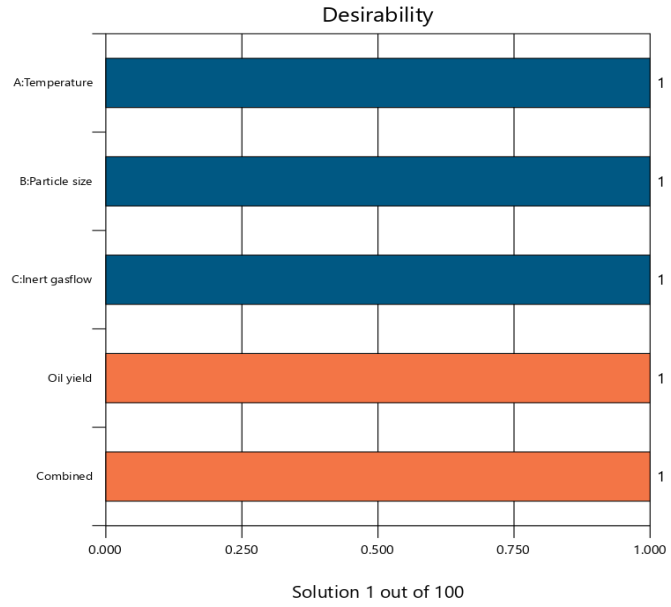

Figure 8: Desirability plot for the yield of bio-oil

Table 7: First 10 solutions for optimization of yield and purity with desirability

Number	Temperature	Particle size	Inert gas flow	Oil yield	Desirability	
1	**461.840**	**3.842**	**1.020**	**31.428**	**1.000**	**Selected**
2	600.000	6.000	1.250	22.644	1.000	
3	500.000	3.500	1.250	27.400	1.000	
4	600.000	1.000	1.250	26.769	1.000	
5	500.000	1.000	1.500	21.769	1.000	
6	600.000	3.500	1.000	30.125	1.000	
7	400.000	3.500	1.000	25.637	1.000	
8	500.000	6.000	1.000	32.331	1.000	
9	400.000	1.000	1.250	16.556	1.000	
10	600.000	3.500	1.500	21.163	1.000	

3.4.1 Model validation

Validation experiments were conducted at the optimal conditions suggested by RSM to confirm the model's reliability. Triplicate experiments were done and average bio-oil obtained was 29.6%. The experimental bio-

Corresponding author's email address: chijiokeugwuodo@mouau.edu.ng

oil yields were in close agreement with the predicted values, with percentage errors less than 10%, demonstrating the model's accuracy in practical applications.

4. Conclusion

This study investigated the pyrolysis of soursop (Annona muricata) seeds in a fixed-bed reactor to optimize bio-oil production and assess its potential as a renewable energy source. The findings highlight that process parameters, like temperature, particle size, and inert gas flow rate, significantly influence bio-oil yield and composition. The optimal conditions for maximizing bio-oil production were determined using Response Surface Methodology (RSM), with a temperature of 461.84°C, a particle size of 3.84 mm, and an inert gas flow rate of 1.02 L/min, yielding 31.43% bio-oil. Characterization of the bio-oil through GC-MS and FTIR analysis confirmed the presence of valuable compounds, including linoleic acid, palmitic acid, and esters, making it a potential feedstock for biofuel production.

The study underscores the viability of soursop seed pyrolysis as an environmentally friendly waste management strategy and a means of generating sustainable biofuels. Additionally, the biochar produced presents opportunities for soil enhancement and carbon sequestration. While this research contributes valuable insights into optimizing bio-oil yield, further studies are recommended to enhance bio-oil stability, refine upgrading techniques, and evaluate large-scale production feasibility. With continued research and technological advancements, bio-oil from soursop seeds could become a viable alternative to conventional fossil fuels, supporting global efforts toward sustainable energy development.

References

Aboelela, D., Saleh, H., Attia, AM., Elhenawy, Y., Majozi, T. and Bassyouni, M. 2023. Recent advances in biomass pyrolysis processes for bioenergy production: Optimization of operating conditions. *Sustainability*, 15(9): 11238–11258. https://doi.org/10.3390/su151411238

Abel, OM., Chinelo, AS., Cynthia, I., and Agbajor, GK. 2020. Evaluation of African star apple (Chrysophyllum albidum) seed oil as a potential feedstock for industrial application. *Asian Journal of Applied Chemistry Research*, 10(4): 31–42.

Adekanmi, DG. and Olowofoyeku, AE. 2020. African star apple: Potentials and application of some indigenous species in Nigeria. *Journal of Applied Sciences and Environmental Management*, 24(8): 1307–1314.

Adibah, W., Azwar, E., Fong, S., Ahmed, A., Peng, W., Tabatabaei, M., Park, Y., and Lam, SS. 2021. Valorization of municipal waste using co-pyrolysis for green energy production, green security, and environmental sustainability: A review. *Chemical Engineering Journal*, 18(7): 129749–129761.

Alkhalidi, HM., Ali, HM., and Jebreen, J. 2023. Characterization of biochar produced from various agricultural wastes and its application in soil improvement. *Environmental Science and Pollution Research*, 30(7): 18125–18135.

Almeida, AP., Tavares, SM., and Silva, FJ. 2021. Application of Design Expert for the optimization of material synthesis processes. *Materials Science and Engineering*, 807(34): 140677-140699.

Anas, A., Noorfidza, Y. H., Sharjeel, W., Ushtar, A., and Syed, AG. 2024. Optimization of Operational Parameters Using Artificial Neural Network and Support Vector Machine for Bio-oil Extracted from Rice Husk. American Chemical Society ACS Omega, 56(13): 254-283. https://doi.org/10.1021/acsomega.4c03131

Antal, MJ. and Grønli, M. 2018. *The art, science, and technology of charcoal production*. Industrial & Engineering Chemistry Research, 42(8): 1619-1640

Amenaghawon, AN., Anyalewechi, CL., Okieimen, CO., and Kusuma, HS. (2021). Biomass pyrolysis technologies for value-added products: A state-of-the-art review. *Environment, Development and Sustainability*, 23(7): 14324–14378.

Attard, TM., Clark, JH., and McElroy, CR. 2020. Recent developments in key biorefinery areas. *Current Opinion in Green and Sustainable Chemistry*, 21(3): 64–74.

Corresponding author's email address: chijiokeugwuodo@mouau.edu.ng

Auburn, A. 2017. Bio-oil Production through Fast Pyrolysis and Upgrading to Green Transportation Fuels. *International Journal of Science and Technology*, 2(9): 650– 657.

Álvarez-Chávez, BJ., Godbout, S., Le Roux, É., Palacios, JH., and Raghavan, V. 2019. Bio-oil yield and quality enhancement through fast pyrolysis and fractional condensation concepts. *Biofuel Research Journal*, 24(8): 1054–1064. https://doi.org/10.18331/BRJ2019.6.4.2

Biswas, B., Singh, R., Kumar, J., and Krishna, BB. 2022. Pyrolysis of Agricultural Biomass Residues: Comparative Study of Fixed Bed and Fluidized Bed Reactors. Bioresource Technology, 34(1): 125805-125845

Balat, M., Kırtay, E., and Balat, H. 2021. *Main routes for the thermo-conversion of biomass into fuels and chemicals*. Part 1: Pyrolysis systems. Energy Conversion and Management, 50(12): 3147-3157.

Belmajdoub, F., and Abderafi, S. 2023. Efficient machine learning model to predict fineness, in a vertical raw meal of Morocco cement plant, Results Eng., 17(5): 100833-100862.

Benn, N., and Zitomer, D. 2018. Pretreatment and anaerobic co-digestion of selected PHB and PLA bioplastics. Front. Environ. Sci., 5(3): 93-113

Boer YD. 2019. Kyoto Protocol to the United Nations Framework Convention on Climate Change. in: *kyoto protocol reference manual on accounting of emissions and assigned amount*, World Book, inc.

Boutin, O., Ferrer, M., and Lédé, J. 2020. *Flash pyrolysis of cellulose pellets submitted toa concentrated radiation: experiments and modelling*. Chemical Engineering Science, 57(1): 15-25.

Bridgwater, A.V. 2012. Review of fast pyrolysis of biomass and product upgrading. *Biomass and Bioenergy*, 38(6): 68–94. https://doi.org/10.1016/j.biombioe.2011.01.048

Bridgwater, T. 2019. *Pyrolysis of Biomass*. IEA Bioenergy: Task 34. Bioenergy Research Group, Aston University, Birmingham, UK

Bridgwater, A., Czernik, S., and Piskorz, J. 2018. *An overview of fast Pyrolysis*. Progress in thermochemical biomass conversion, 54(11): 977-997

Bramer, E., and Holthuis, M. 2018. *Clean liquid fuel through flash pyrolysis*. The Development of the PyRos Process, 10(1): 104-132

Bridgwater, A., and Peacocke, G. 2019. *Fast pyrolysis processes for biomass*. Renewable and sustainable energy reviews, 4(1): 1-73.

Dajanta, P., Bhuiyan, MM., and Yusof, N. 2021. Influence of pyrolysis temperature on the yield and properties of biochar from soursop seeds. *Journal of Cleaner Production*, 278(15): 123-146.

Demirbaş, A**.** (2004). Combustion characteristics of different biomass fuels. *Progress in Energy and Combustion Science*, 30(2): 219–230. https://doi.org/10.1016/j.pecs.2003.10.004

Dina, A., Habibatallah, S., Attia MA., Yasser, E., Thokozani, M. and Mohamed, B. 2023. Recent Advances in Biomass Pyrolysis Processes for Bioenergy Production: Optimization of Operating Conditions. Journal Sustainability, 15(5): 11238-11268. https://doi.org/10.3390/su151411238.

Fakhari, SM., Mrad, H. 2023. Optimization of an axial-flow mine ventilation fan based on effects of design parameters, Results in Engineering, 42(9): 101662-101690.

González, M., Gómez, C., and López, J. 2021. Statistical optimization of extraction processes using Design Expert: A review. *Journal of Food Engineering*, 284(22): 110136-110161.

Hilal, DA. 2018. *Yields and heating values of liquids and chars from spruce trunk bark pyrolysis*. Energy sources, 27(14): 1367-1373.

Hofmann, L., and Antal, MJ. 2022. *Numerical simulations of the performance of solar fired flash pyrolysis reactors*. Solar energy, 33(5): 427-440

Corresponding author's email address: chijiokeugwuodo@mouau.edu.ng

Hossain, A., Hasan, MR., and Islam, MR. 2018. *Design, fabrication and performance study of a biomass solid waste pyrolysis system for alternative liquid fuel production*. Global Journal of Researches in Engineering, 14(5): 115-142

Hossain, AK. and Davies, PA. 2013. Pyrolysis liquids and gases as alternative fuels in internal combustion engines–A review. *Renewable and Sustainable Energy Reviews,* 21(5): 165-189. https://doi.org/10.1016/j.rser.2012.12.031

Huang, YF., Chiueh, PT. and Kuan, WH. 2021. Review on catalytic Pyrolysis of biomass for biofuels production. Energy Conversion and Management, 156(4): 1-15.

Ingle, AI., Shashikala, HD., Narayanan, MK., Dubeto, MT. and Gupta, S. 2023. Optimization and analysis of process parameters of melt quenching technique for multiple performances of rare earth doped barium borate glass synthesis using Taguchi's design and grey relational approach, Results Eng., 17(7): 100784-100802.

Ishaq, M., Ullah, S. and Abbas, M. 2020. Valorization of agricultural residues: Biochar and bio-oil production from soursop seeds. *Waste Management*, 102(12): 116-124.

Kan, T., Strezov, V. and Evans, T. J. 2016. Lignocellulosic biomass pyrolysis: A review of product properties and effects of pyrolysis parameters. *Renewable and Sustainable Energy Reviews, 57*(8): 1126-1140. https://doi.org/10.1016/j.rser.2015.12.185

Lam, SS., Russell, AD. and Chase, HA. 2019. Microwave pyrolysis, a novel process for recycling waste automotive engine oil. Energy, 35(7): 2985-2991.

Lehmann, J., and Joseph, S. 2019. Biochar for Environmental Management: Science, Technology, and Implementation. Routledge., 67(4) 236-261.

Li, X., Grace, J., Lim, C., Watkinson, A., Chen, H., and Kim, J. 2019. *Biomass gasification in a circulating fluidized bed*. Biomass and Bioenergy, 26(2): 171-193.

Lv, P., Xiong, Z., Chang, J., Wu, C., Chen, Y. and Zhu, J. 2019. *An experimental study on biomass air– steam gasification in a fluidized bed*. Bio-resource technology, 95(1): 95-101.

Mansur, MB., Mohd, SR., and Rahman, MS. 2020. Potential of agricultural waste biomass as a renewable energy source: A case study of soursop seeds. *Renewable Energy*, 145(3): 2154-2160.

Martínez, JJ., Rojas, MI. and Amaya, DB. 2020. Nutritional and health-promoting properties of soursop (Annona muricata L.). *Food Research International*, 137(7): 109508-109529.

Miandad, R., Barakat, MA., Aburiazaiza, AS., Rehan, M. and Nizami, AS. 2016. Catalytic pyrolysis of plastic waste: A review. *Process Safety and Environmental Protection*, 102(10): 822–838. https://doi.org/10.1016/j.psep.2016.06.022

Mohan, D., Pittman, CU., and Steele, PH. 2021. Pyrolysis of Wood/Biomass for Bio-oil: A Critical Review. Energy & Fuels, 20(3): 848-889.

Montgomery, DC. (2019). *Design and Analysis of Experiments*. Wiley.

Narayan, LP. and Arjun, SP. 2021. An overview of recent development in bio-oil upgrading and separation techniques. Environ. Eng. Res., 26(5): 200382-200398 https://doi.org/10.4491/eer.2020.382

Nwosu-obieogu, K., Ezeugo, J., Onukwuli, OD. and Ude, CN. 2024. Modelling and optimizing the transesterification process of shea butter via CD-BaCl-IL catalyst using soft computing algorithms. Results in Engineering, 22(4): 102004-102031.

Okeleye, AA. and Betiku, E. 2019. Kariya (Hildegardia barteri) seed oil extraction: comparative evaluation of solvents, modeling, and optimization techniques, Chem. Eng. Commun., 206 (9): 1181–1198.

Okokpujie, IP., Anthony, OO., Ejiroghene, O., Kunle, B., Emmanuel, SAA., Christian, OO., Stephen, AA., Esther TA. 2023. Modelling and optimization of intermediate pyrolysis synthesis of bio-oil production from palm kernel shell. Cleaner Engineering and Technology, 16(2): 100672-100692.

Corresponding author's email address: chijiokeugwuodo@mouau.edu.ng

Onaifo, GO., Omoriyekomwan, JE. and Shadare, OA. 2023. Co-pyrolysis of soursop and mango seeds for bio-oil production. *Biomass Conversion and Biorefinery*, 43(2): 342-364. https://doi.org/10.1007/s42250-022-00536-9.

Pedro, HCS., Sônia, DFR. and Daniel, BR. 2022. Luffa cylindrica Slow Pyrolysis and Solar Pyrolysis: Impact of Temperature and Heating Rate on Biochar Properties and Iodine Adsorption Performance. Research Square, 106(3): 304-331. https://doi.org/10.21203/rs.3.rs-1497697/v1

Saravanakumar, MP., Sulaiman, SA., Lam, SS., Abdullah, N. and Suganya, OM. 2021. Pyrolysis kinetics of lignocellulosic biomass and bio-oil properties: A comprehensive review. Energy Conversion and Management, 242(8): 114330-114354. doi:10.1016/j.enconman.2021.114330

Schroeder, LR., Barros, JC., and Silva, AM. 2017. Chemical and physical analysis of liquid fractions from soursop seed cake pyrolysis. *Journal of Analytical and Applied Pyrolysis,* 124(6): 493-500. https://doi.org/10.1016/j.jaap.2017.02.005

Singh, A., Kumar, A., and Kumar, P. 2021. Pyrolysis of agricultural waste for bioenergy production: A review. *Renewable and Sustainable Energy Reviews*, 135(1): 110199-110216.

Soria-Verdugo, A., Bongers, L., Serna-Guerrero, R., Oliva-Buitimea, J. and Nájera, O. 2020. Review of biomass pyrolysis oils properties and upgrading technologies: Recent advances and future prospects. Journal of Analytical and Applied Pyrolysis, 148(24): 104819-104843. doi:10.1016/j.jaap.2020.104819

Sonntag, A. 2012. Reaction of fats and fatty acids. In: Balley (Eds) industrial oil and fat Products, fourth ed wiley, New York USA, 23(9): 99–120

Sharma, R., Agarwal, A. and Kumar, S. 2020. Optimization of extraction processes for bioactive compounds using Design Expert. *Journal of Cleaner Production*, 253(12): 119964-119986.

Sharma, RK., Wooten, JB., Baliga, VL., Lin, X., Chan, WG., and Hajaligol, M. R. 2021. Characterization of chars from Pyrolysis of lignin. Fuel, 83(11-12): 1469-1482.

Tripathi, M., Sahu, JN., and Ganesan, P. 2021. Fixed Bed Pyrolysis of Biomass: A Review. Journal of Renewable and Sustainable Energy, 5(4): 53402-53420.

Ude, CN., Onukwuli, OD., Ugwu, BI., Okey-Onyesolu, CF., Ezidinma, TA. and Ejikeme, PM. (2020). Methanolysis optimization of cottonseed oil to biodiesel using heterogeneous catalysts. Iran. J. Chem. Chem. Eng., 39(4): 355-370.

Ude, CN., Christopher, NI., Nwosu-Obiego, K., Patrick, CN., Collins, NO., Ndidi, FA., Cordelia, NE., and Uchenna, CO. 2023. Optimization of dual transesterification of jatropha seed oil to biolubricant using hybridized response surface methodology (RSM) and adaptive neuro fuzzy inference system (ANFIS)-genetic algorithm (GA). Sustainable Chemistry for the Environment 4(2): 100050-100072. https://doi.org/10.1016/j.scenv.2023.100050

Wang, Y., Liu, H., Lv, Y., Wang, J., Gu, X. and Zhang, M. 2022. Effects of combined applications of biochar and chemical fertilizer on crop yield, soil organic carbon, and crop quality of a rice-wheat rotation system in China. Agriculture, Ecosystems & Environment, 287(12): 106687-106709. doi:10.1016/j.agee.2019.106687

Corresponding author's email address: chijiokeugwuodo@mouau.edu.ng